Measurement of double differential cross sections for fragment-production induced by tens of MeV particles.

M. Hagiwara, M. Baba, T. Oishi,
Cyclotron and Radioisotope Center, Tohoku University
E-mail: *hagi@cyric.tohoku,ac,jp*
T. Sanami
High Energy Accelerator Research Organization (KEK)
H. Nakashima, S. Tanaka
Japan Atomic Energy Research Institute
M. Takada
National Institute of Radiological Sciences

Measurements of differential fragment production cross sections for proton- and neutron-induced reaction are described. Double-differential fragment production cross section for 70 MeV protons and the yields for 65 MeV neutrons were obtained with a specially designed Bragg curve spectrometer (BCS). An experiment is also described for proton-induced reactions employing the E-TOF method to obtain complementary and more detailed information than neutron-induced reactions.

1. INTRODUCTION

Fragments which are secondary particles heavier than alpha-particle, cause a large local ionization. It is a serious problem for a semiconductor device and human in space environment. Therefore, the data for fragments production, in particular, the energy and angular doubly differential cross-section data (DDX) are required for dosimetry and evaluation of radiation effects in devices or instruments, such as single event upset (SEU) by cosmic rays. Up to now, however, experimental data of the fragment production are very scarce due to experimental difficulties of the detection. Thus, almost all past experimental data were obtained by the activation method that did not provide energy and angle information. Furthermore, theoretical calculation treating fragment production is very few. Therefore, it is important to accumulate reliable experimental DDX data for fragment production.

For fragment detection, we adopted 1) a Bragg curve spectrometer (BCS) providing various information with a single counter and 2) an energy-time of fight (E-TOF) method having the capability of mass identification in almost whole energy region for fragment. For 1), BCS was designed with special care to apply to a neutron beam, in addition to a charged particle beam and resulted in success to obtain light fragments by proton- and neutron-induced reactions. BCS proved very promising for fragments detection in neutron-induced reaction, while there are still some problems that should be solved. For 2), we have fabricated a chamber for measurements and started measurements.

This paper describes energy-angular fragment production measurements in neutron- and proton-induced reactions and experimental plan of extension to proton-induced reactions employing the energy and TOF method (E-TOF) method.

2. BRAGG CURVE SPECTROMETER (BCS)

2.1 Principle of BCS

Figure 1 shows a schematic diagram of BCS. It is a cylindrical gridded ionization chamber (GIC). The distance between the cathode and the grid is 27 cm, the grid and the anode is 0.5 cm. Wire radius and spacing of

the grid are 0.1mm and 1mm, respectively. Thus, the grid inefficiency is 2.6 %. Ring electrodes are arranged in 3 cm steps to achieve a homogeneous electric field. The chamber is filled with an Ar + 10%CH_4 gas at a pressure of 2.7×10^4 Pa (200 Torr). As shown in fig 2, if fragments enter the detector along the axis through a thin film window and ionize the gas in BCS, ionized electrons drift to the anode by the electric field keeping a shape of Bragg curve. The time distribution of the anode signal corresponds to the reversal of the ionization distribution (Bragg curve) by the fragment. Therefore the fast part of anode signal is proportional to the Bragg peak value that is in proportion to the atomic number (Z) of the fragment. The integration of the whole anode signal represents the total charge that is proportional to the fragment energy. Therefore, BCS can provide information on the energy and the atomic number of fragments using only the anode signal.

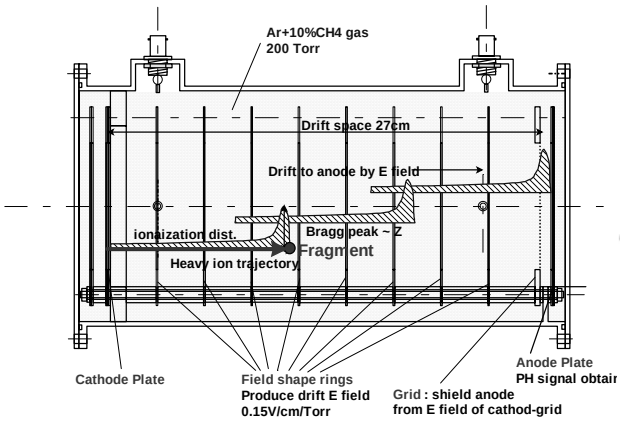

Fig.1 Schematic diagram of the Bragg curve spectrometer

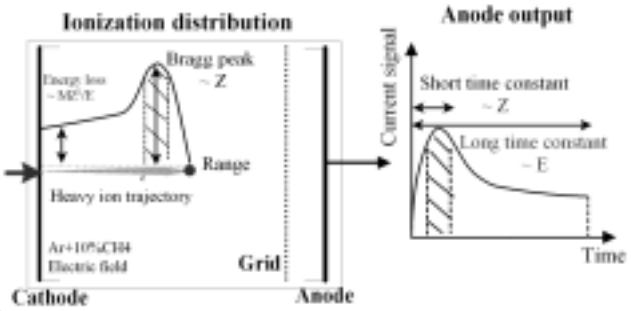

Fig. 2 Detection scheme of BCS method

To apply BCS to neutron-induced reactions, we put samples inside the chamber to decrease the energy loss of fragment and enlarge the detection solid angle. In this case, however, the following difficulties arise:

1) increase of backgrounds due to neutron irradiation of the chamber body and detection gas, and

2) distortion of anode signal due to angular spread of fragments.

To solve 1) we adopt tight neutron collimation, high-Z element electrodes having small fragment production rate, and an additional shield electrode. The shield electrode is installed in front of the chamber with the same potential as the cathode, to reject signals by charged particles from chamber wall in front of the cathode plate.

The problem 2) will be solved by using the above geometrical arrangement and employing the cathode signal which has dependence on the angle relative to the BCS axis [4, 5].

3. APPLICATION OF BCS TO PROTON-INDUCED REACTION

Figure 3 shows the experimental setup used in the case of proton-induced reaction at the cyclotron laboratory of National Institute of Radiological Science. The fragments emitted to 30 degree direction were measured. The proton energy was 70 MeV. Proton beam current was ~10 nA. For samples, foils of carbon 100 μm thick, and silicon 500 μm thick, aluminum 2 μm thick, and polypropylene 4 μm thick were employed.

Figure 4 shows the electronics block diagram used in a series of experiments. In this circuit, the energy signal and the Bragg peak signal were obtained from the anode signal by processing with a long time constant (6 μsec) and a short time constant (0.25 or 0.5 μsec), respectively. To reduce background events and dead time of ADC, only coincidental data between anode and cathode were accumulated by using 4F1V and GG (See fig. 4). The coincidence time is set to 6 μsec that is equivalent to the maximum traveling time of electrons from the cathode to grid. They are collected as a two-dimensioned data by KODAQ (Kakuken Online Data Acquisition System) [6] with CAMAC system.

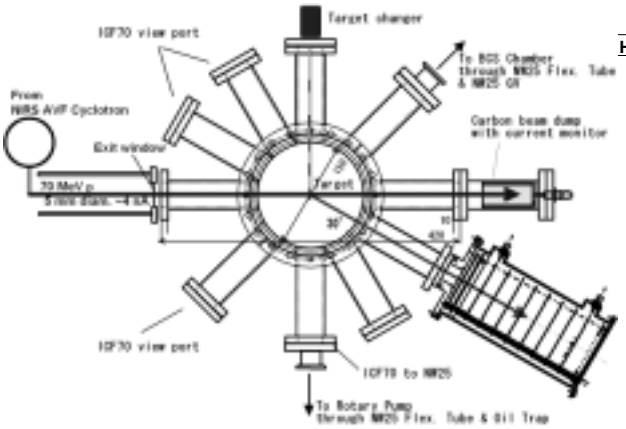

Fig. 3 The block diagram of electronics circuit

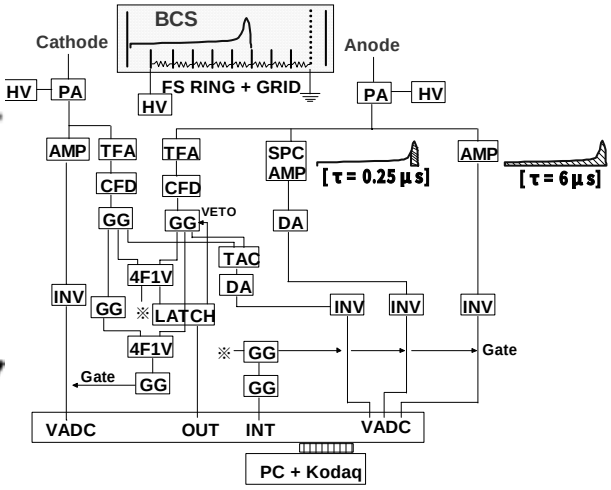

Fig. 4 The block diagram of electronics circuit

Figure 5 shows the measured two-dimensional spectrum on the energy *vs.* Bragg peak. Excellent separation of each fragment and S/N ratio are confirmed in the energy region where particles are separated as shown in fig.6. In this case, fragments lighter than carbon are produced mainly and heavier products are very few. The turning blows at maximum energy point in fig. 5 are caused by the fragments that have ranges longer than the cathode-grid distance. It is meaningful to extend the measurable energy range by developing a correction method for this effect. Energy calibration was performed by replacing a sample with ^{241}Am α source. The DDX for lithium, beryllium and boron from carbon obtained by polypropylene sample are shown in figs. 7-9. As observed in fig.7, the present results agree with the data by C. T. Roche [8] et al. in shape.

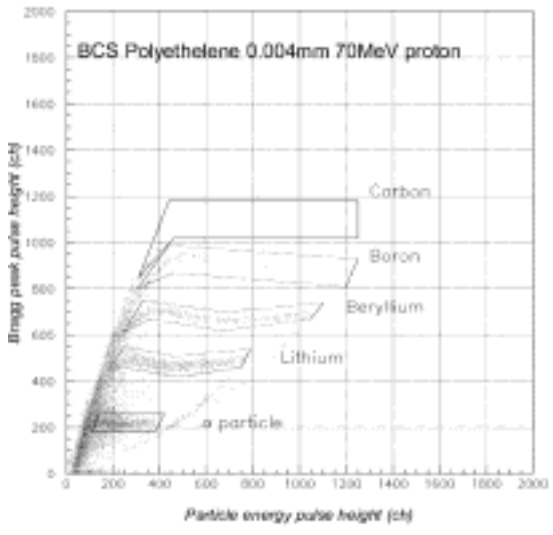

Fig. 5 the energy *vs* Bragg peak two-dimensional spectra for polypropylene 4 μm sample

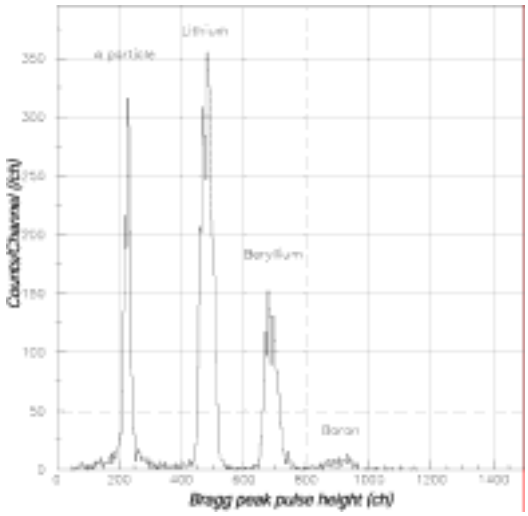

Fig. 6 the histogram of Bragg peak over separation limits for polypropylene 4 μm sample

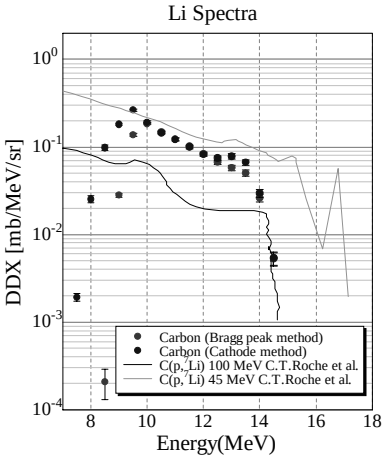

Fig. 7 Lithium spectra

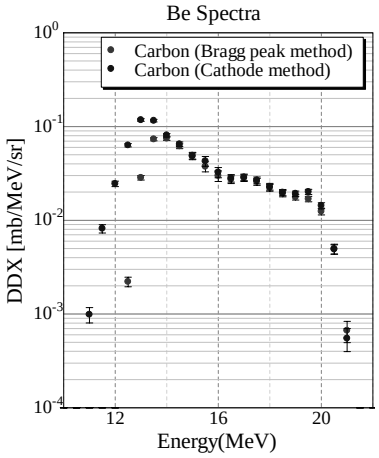

Fig. 8 Beryllium spectra

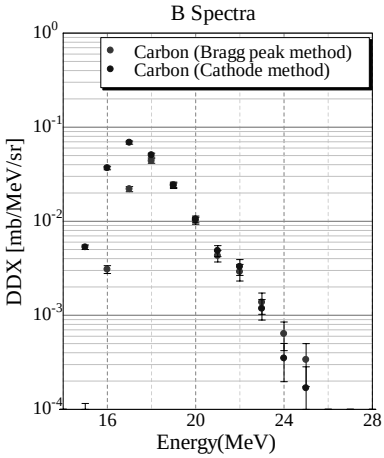

Fig. 9 Boron spectra

4. APPLICATION OF BCS TO NEUTRON-INDUCED REACTION

4.1Experimental setup

An experiment for neutron-induced reaction was performed using the ^{7}Li(p,n) neutron source at TIARA, JAERI, Takasaki site. To measure fragments from carbon, samples of carbon 100 μm thick, 200 μm thick, and nickel 100 μm thick, aluminum 6 μm thick were employed. Each sample set on the cathode plate inside was irradiated directly by neutrons collimated by a ~3 m long neutron collimator, and ~60 cm long additional collimator to avoid neutrons hitting the BCS structure. The proton energy was 70 MeV and the neutron peak energy was ~65 MeV [7]. Proton beam current was ~1 μA. Nickel and thin aluminum samples were used to evaluate the backgrounds originated from BCS gas and entrance window, respectively. This application might be the first trial to neutron-induced reaction in the world.

4.2 Result

Figure 10 shows the two-dimensional spectrum on the energy *vs.* Bragg peak for neutron-induced reaction on a 200 μm-thick carbon sample. The spectrum was obtained by only ~4 hour irradiation. The electronics circuit is the same as fig. 5. Fragments heavier than α particle are separated distinctly as shown in fig. 11, though the separation of Bragg peak was not better compared with proton-induced reaction. Hydrogen isotopes are eliminated by the electronics because of small energy loss in the chamber.

The energy spectra for each sample are shown in figs. 12-14. As observed in these figures the results of two carbon samples are in fair agreement. It will be due to the fact that the range of fragments in carbon (~several μm) is much shorter than sample thickness. These samples are too thick compared with fragment ranges but the spectra obtained were close to that from a thin sample. The yields for the nickel sample are lowest for all fragments because of smaller cross-sections for fragment emission than carbon and aluminum. The data for the thin aluminum sample are similar as the nickel case in magnitude and suggest that the data for nickel and aluminum are close to backgrounds. The lower limit of the spectrum (α particle: 2 MeV, carbon: 8 MeV) is governed by the particle identification limit of BCS and the upper limit by the range of the particle in the gas (α particle: 7.5 MeV, carbon: 38 MeV). We are considering to extend the dynamic range by treating the overlap at lower energy and blow in high energy end. For the purpose, improvement of BCS for more tight geometry and sample-changing mechanism, and also application of digital signal processing using a high speed digital oscilloscope are now in progress.

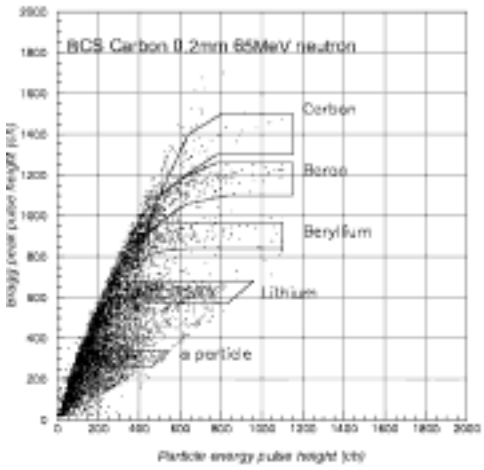

Fig. 10 the energy *vs* Bragg peak two-dimensional spectra for carbon 200 μm sample

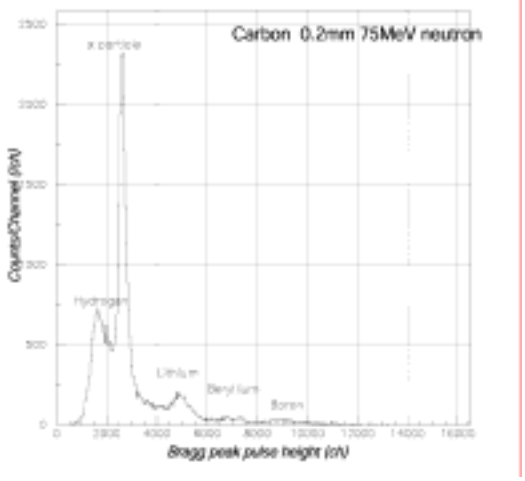

Fig. 11 the histogram of Bragg peak over separation limits for carbon 200 μm sample

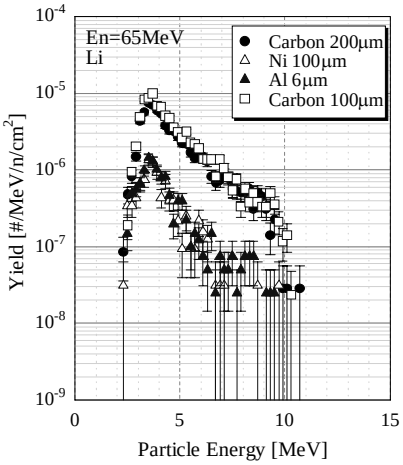

Fig. 12 Lithium spectra

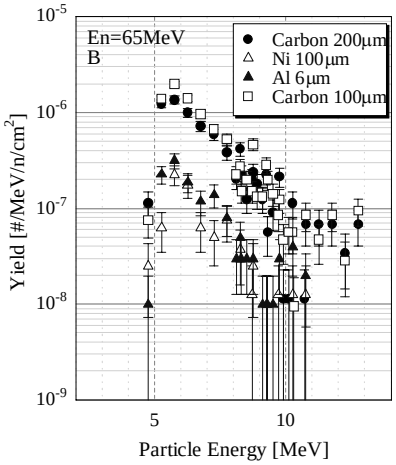

Fig. 13 Beryllium spectra

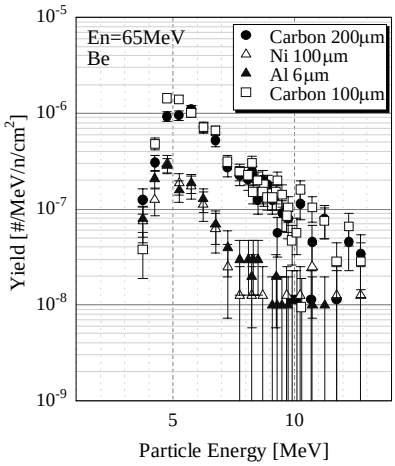

Fig. 14 Boron spectra

5. Fragment production experiment for proton-induced reactions with E-TOF method

In the case of neutron induced reaction, there are several difficulties such as 1)low counting rate, high backgrounds due to neutron bombardment of BCS body, and 3) non-monoenergetic neutron source and so on. We are now planning to do fragment measurement for proton-induced reactions using a energy-TOF method which is used in heavy ion detection. In this method, the energy and TOF of the fragment is measured and mass and atomic number are derived by combing the energy, TOF and energy loss information. Therefore, the dynamic range of fragment energy will be higher than in BCS, and much higher counting rate will be obtained. These data will be useful to complement neutron-induced data. Furthermore, the fragment production data for proton induced reaction are important and useful for analysis of soft errors around accelerators and in space. For the reason, we fabricated a chamber for proton-induced fragment measurement and are stating experiments. The schematic view of the chamber is shown in Fig.15.

For a start detector of TOF, we will employ a MCP (micro-channel plate) coupled with a thin Al film which has good time resolution and low energy loss for fragments. For a stop detector (E detector), MCP and SSD

which has good energy resolution will be adopted. The scattering chamber was designed to enable simultaneous measurements of BCS and E-TOF. The combination of these methods will be powerful for the measurement of fragments induced by charged particles.

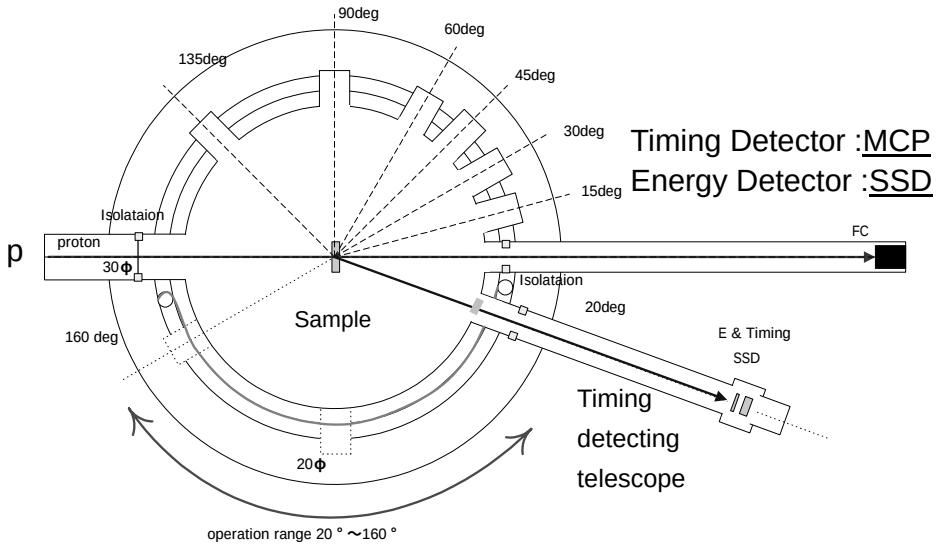

Fig.15 Schematic view of vacuum chamber for E-TOF measurement

6. SUMMARY

We developed a BCS detector and applied to proton- and neutron-induced reactions aiming at measurement of fragment production cross section. Through the experiments, BCS proved to be applicable to neutron-induced reaction. We intend to improve the measuring method with the refinement of data treatment as follows employing new data acquisition method:

1) evaluation and decrease of backgrounds,
2) extension of the dynamic range, and
3) correction for the effects of emission angle.

We are also preparing fragment production measurement for proton-induced reactions using the energy-TOF technique to extend energy range and improve data quality.

ACKNOWLEDGEMENT

The authors express their thanks to the operation crew of the NIRS cyclotron and TIARA cyclotron for their cooperation.

REFERENCES

(1) C.R.Gruhn, et al. *Nucl. Instrum. Methods*, **196** (1982) 33.
(2) N.J.Shenhav and H.Stelzer, *Nucl.Instrm.Meth.* **228** (1985) 359
(3) O.Bunemann, et al., *Can. J. Res.* **A27** (1949) 373
(4) N.Ito, M.Baba, et al., *Nucl.Instrum.Meth.* **A337** (1994) 474
(5) T.Sanami, et al. *Nucl. Instrum. Meth.* **A440** (2000) 403.
(6) K.Omata et al., INS-Rep-884, Institute for Nuclear Study, University of Tokyo, 1991
(7) M.Baba et al. *Nucl. Instrum. Meth.* **A428** (1999) 454
(8) C.T.Roche et al. Phys. Rev. C **14** (1976) 410